

Supporting Information

**A rotaxane-based platform for tailoring the pharmacokinetics of cancer-targeted
radiotracers**

Faustine d'Orchymont and Jason P. Holland*

University of Zurich, Department of Chemistry, Winterthurerstrasse 190, CH-8057, Zurich, Switzerland

*** Corresponding Author:**

Prof. Dr Jason P. Holland

ORCID: orcid.org/0000-0002-0066-219X

Tel: +41-44-63-53990

E-mail: jason.holland@chem.uzh.ch

Website: www.hollandlab.org

Twitter: @HollandLab_

First Author:

Dr Faustine d'Orchymont

ORCID: orcid.org/0000-0002-3726-1648

E-mail: faustine.dorchymont@chem.uzh.ch

Table of Contents

<i>Methods</i>	4
Chemicals and solvents	4
NMR spectroscopy	4
Mass spectrometry	4
High-performance liquid chromatography	4
Size-exclusion chromatography (SEC)	5
Radioactivity	5
Quantification of radioactivity	6
Photochemistry	6
Cell culture	6
Immunoreactivity (Lindmo-type cell binding assay)	7
Animals and xenograft models	7
Small-animal positron emission tomography (PET) imaging	7
PET image quantification by volume-of-interest (VOI) analysis	8
Biodistribution studies (ex vivo)	8
Effective half-life measurements	8
Statistical analysis	9
<i>Synthesis and Characterisation</i>	9
Radiosynthesis of [⁸⁹ Zr]Zr-1	10
Figure S1. Radio-TLC chromatograms for [⁸⁹ Zr]Zr-1 (orange) in 50 mM DTPA and the associated control sample, [⁸⁹ Zr][Zr(DTPA)] ⁻	10
Photoradiosynthesis of [⁸⁹ Zr]ZrFe-[4]rotaxane-azepin-onartuzumab, [⁸⁹ Zr]ZrFe-2	11
Scaled-up photoradiosynthesis of [⁸⁹ Zr]ZrFe-[4]rotaxane-azepin-onartuzumab for biological experiments	11
Figure S2. Preparative Sephadex G100-SEC profiles for the purification of [⁸⁹ Zr]ZrFe-[4]rotaxane-azepin-onartuzumab (n = 3, green) and with a scale-up of the activity for animal experiments (black)	12
Figure S3. Size-exclusion (G100) chromatogram of [⁸⁹ Zr]ZrFe-2 after incubation in the formulation buffer for 72 h at ambient conditions.	12
Figure S4. Cellular binding (Lindmo) assay on [⁸⁹ Zr]ZrFe-[4]rotaxane-azepin-onartuzumab.	13
Animal studies and preparation of [⁸⁹ Zr]ZrFe-[4]rotaxane-azepin-onartuzumab doses for injection in mice	13
Figure S5. Maximum intensity project (MIP) [⁸⁹ Zr]ZrFe-2 PET images of a representative mouse from the normal (top) and blocking (bottom) group.	14
Figure S6. Time-activity curves (TACs) obtained from quantitative volume-of-interest (VOI) analysis from the normal (n = 5), and (g) the blocking (n = 5) group of animals illustrating the tumour specificity of [⁸⁹ Zr]ZrFe-2.	15
Table S1. Quantitative data from the VOI analysis of the PET images.	15
Biodistribution results	16
Table S2. Ex vivo biodistribution data measured at 72 h after i.v. administration of [⁸⁹ Zr]ZrFe-[4]rotaxane-azepin-onartuzumab (normal and blocking groups) in female athymic nude mice bearing subcutaneous MKN-45 tumours.	16
Preparation of [⁸⁹ Zr]ZrFe-[4]rotaxane-2-hydroxyazepin [⁸⁹ Zr]ZrFe-3	16

Synthesis of the [3]pseudorotaxane 4 and the [3]rotaxane ^{nat} Zr-4	17
Figure S7. Reverse-phase analytical HPLC chromatogram of complex 4, λ= 254 nm.	17
Figure S8. HRMS (ESI+) spectrum of compound 4.....	18
Figure S9. ¹ H NMR of compound 4 (D ₂ O, 500 MHz).....	18
Figure S10. ¹³ C{ ¹ H} NMR of compound 4 (D ₂ O, 126 MHz).	19
Figure S11. DEPT-135 of compound 4 (D ₂ O).	19
Figure S12. DEPT-90 of compound 4 (D ₂ O).	20
Figure S13. HSQC of compound 4 (D ₂ O).....	20
Figure S14. HMBC of compound 4 (D ₂ O).....	21
Figure S15. Reverse-phase analytical HPLC chromatogram of complex ^{nat} Zr-4, λ= 254 nm.....	22
Figure S16. HRMS (ESI+) spectrum of compound ^{nat} Zr-4.....	22
Radiosynthesis of [⁸⁹ Zr]ZrFe-4	22
Figure S17. Radio-iTLC [⁸⁹ Zr]ZrFe-4 (blue), and [⁸⁹ Zr]Zr-DTPA (black) as a control.	23
Effective half-life measurements	23
Figure S18. One-phase model for the experimentally measured effective half-life of (A) [⁸⁹ Zr]ZrFe-3 (n = 3) and (B) [⁸⁹ Zr]ZrFe-4 (n = 4).	23
Figure S19. Two-phase excretion model for the experimentally measured effective half-life of [⁸⁹ Zr]ZrFe-3 (green) and [⁸⁹ Zr]ZrFe-4 (red).	24
Biodistribution results	24
Table S3. Ex vivo biodistribution data measured at 24 h after i.v. administration of [⁸⁹ Zr]ZrFe-3 and [⁸⁹ Zr]ZrFe-4 in female athymic nude mice.	24
References.....	25

Methods

Chemicals and solvents

Unless otherwise stated, all other chemicals were of reagent grade and purchased from Sigma Aldrich (St. Louis, MO), Merck (Darmstadt, Germany), Tokyo Chemical Industry (Eschborn, Germany), abcr (Karlsruhe, Germany) or CheMatech (Dijon, France). Water ($>18.2 \text{ M}\Omega\cdot\text{cm}$ at 25°C , Milli-Q® Direct 8/16 System, Milipore, Molsheim, France). Solvents for reactions were of reagent grade, and where necessary, were dried over molecular sieves. Solvent evaporation was performed under reduced pressure by using a rotary evaporator (Rotavapor R-300, Büchi Labortechnik AG, Flawil, Switzerland).

NMR spectroscopy

^1H and ^{13}C NMR spectra were measured in deuterated solvents on a Bruker AV-400 (^1H : 400 MHz, ^{13}C : 100.6 MHz) or a Bruker AV-500 (^1H : 500 MHz, ^{13}C : 125.8 MHz) spectrometer. Chemical shifts (δ) are expressed in parts per million (ppm) relative to the resonance of the residual solvent peaks, for example, with DMSO $\delta_{\text{H}}=2.50$ ppm and $\delta_{\text{C}}=39.5$ ppm with respect to tetramethylsilane (TMS, δ_{H} and $\delta_{\text{C}} = 0.00$ ppm). Coupling constants (J) are reported in Hz. Peak multiplicities are abbreviated as follows: *s* (singlet), *d* (doublet), *dd* (doublet of doublets), *t* (triplet), *q* (quartet), *m* (multiplet), and *b* (broadened). Two-dimensional NMR experiments including ^1H - ^1H correlation spectroscopy (COSY), ^{13}C - ^1H heteronuclear single quantum coherence (HSQC) and ^{13}C - ^1H heteronuclear multiple bond correlation (HMBC) were performed to aid the assignment of the ^1H and ^{13}C spectra.

Mass spectrometry

High-resolution electrospray ionisation mass spectra, HRMS (ESI), and high-resolution electron impact ionisation mass spectra, HRMS (EI), were measured by the mass spectrometry service at the Department of Chemistry, University of Zurich.

High-performance liquid chromatography

Semi-preparative high-performance liquid chromatography (HPLC) was performed on a Rigol L-3000 system (Contec AG, Switzerland) equipped with a UV-Vis (absorption measured at 220 nm and 254 nm), fitted with a reverse-phase VP 250/21 Nucleodur C18 HTec (21 mm ID \times 250 mm, 5 μm) column. For all HPLC performed, solvent A = $18.2 \text{ M}\Omega\cdot\text{cm H}_2\text{O}+0.1\%$ TFA and solvent B = MeOH and the method used a flow-rate of 7 mL min^{-1} with a linear gradient of A: $t = 0 \text{ min } 5\% \text{ B}$; $t = 30 \text{ min } 100\% \text{ B}$; $t = 40 \text{ min } 100\% \text{ B}$.

Analytical high-performance liquid chromatography (HPLC) experiments were performed by using Hitachi Chromaster Ultra Rs systems fitted with a reverse phase VP 250/4 Nucleodur C18 HTec (4 mm

ID × 250 mm, 5µm, Macherey-Nagel, Düren, Germany) column. This system was also fitted to a FlowStar² LB 514 radioactivity detector (Berthold Technologies, Zug, Switzerland) equipped with a 20 µL PET cell (MX-20-6, Berthold Technologies) for analysing radiochemical reactions. For all HPLC chromatograms shown, solvent A = 18.2 MΩ·cm H₂O+0.1% TFA and solvent B = MeOH and the method used a flow-rate of 0.7 mL min⁻¹ with a linear gradient of A: $t = 0$ min 5% B; $t = 1$ min 5% B; $t = 10$ min 100% B; $t = 11$ min 100% B.

Size-exclusion chromatography (SEC)

Two SEC methods were used. The first method used a size-exclusion column (BioRad Laboratories, ENrich SEC 70, 10±2 µm, 10 mm ID × 300 mm) connected to an automated HPLC device (Rigol L-3000, Contrec AG, Switzerland) equipped with a UV-Vis (absorption measured at 280 nm and/or 430 nm) and an in-line radioactivity detector (FlowStar² LB 514, Berthold Technologies, Zug, Switzerland). Isocratic elution with phosphate buffered saline (PBS, pH7.4) was used for all SEC-HPLC analyses (flow-rate = 1 mL min⁻¹). The second method used manual SEC employing either a PD-10 desalting column (Sephadex G-25 resin, 85–260 µm, 14.5 mm ID × 50 mm, >30 kDa, GE Healthcare) or a custom-made SEC column with the same geometry as the PD-10 columns but employing SephadexTM G-100 media for more efficient separation of the high molecular weight protein fraction from the small-molecule byproducts. For analytical procedures, manual G-100 SEC columns were eluted with sterile PBS. A total of 50×200 µL fractions were collected up to a final elution volume of 10 mL. Manual SEC columns were also used for preparative purification and reformulation of radiolabelled protein samples (sterile PBS, pH7.4).

Radioactivity

Caution: Zirconium-89 ($t_{1/2} = 78.41$ h, $E_{\max}(\beta^+) = 902$ keV, $I(\beta^+) = 22.74\%$, $E_{\gamma} = 909.2$ keV [$I = 99.0\%$], 511.0 keV [$I = 45.5\%$]) emits positrons and high-energy gamma rays. All operations must be performed by qualified personnel in an approved facility and following safety guidelines set forth by the local authorities, and the Nuclear Regulatory Commission. Experimental manipulations should first be practised with non-radioactive samples and researchers should follow the ALARA (As Low As Reasonable Achievable) protocols to minimise exposure to ionising radiation.

Zirconium-89

[⁸⁹Zr][Zr(C₂O₄)₄]⁴⁻(aq.) (also known as ⁸⁹Zr-oxalate) was obtained as a solution in ~1.0 M oxalic acid from PerkinElmer (Boston, MA, manufactured by the BV Cyclotron VU, Amsterdam, The Netherlands) and was used without further purification. Stock solutions of [⁸⁹Zr][Zr(C₂O₄)₄]⁴⁻ were prepared on several occasions by using the same procedure. As an example, a stock solution of [⁸⁹Zr][Zr(C₂O₄)₄]⁴⁻ was prepared by adding ⁸⁹Zr radioactivity from the commercial source (309.7 MBq, 200 µL in ~1.0 M aqueous oxalic acid; PerkinElmer) to an Eppendorf tube. A volume of 100 µL was neutralised by the addition of aliquots of 1.0 M Na₂CO₃(aq) (total volume of 225 µL added, final pH~8.3, final volume ~325 µL, final

activity = 150.1 MBq). Caution: Acid neutralization with Na_2CO_3 releases $\text{CO}_2(\text{g})$ and care should be taken to ensure that no radioactivity escapes the microcentrifuge tube. After CO_2 evolution ceased, the neutralised solution was allowed to equilibrate to room temperature before using the stock solution in ^{89}Zr -labelling reactions.

Unless otherwise stated, ^{89}Zr -labelling reactions were performed at room temperature at pH7–8.5. Radioactive reactions were monitored by using radio-TLC. Glass-fibre TLC plates were developed by using DTPA (50 mM, pH7.4) as the eluent, and were analysed on a radio-TLC detector. RCC was determined by integrating the data obtained by the radio-TLC plate reader and determining both the percentage of radiolabelled product (retention factor, $R_f = 0.0\text{--}0.1$) and 'free' ^{89}Zr ($R_f = 0.9\text{--}1.0$; present in the analyses as $[\text{}^{89}\text{Zr}][\text{Zr}(\text{DTPA})]^-$). Small-molecule ^{89}Zr -radiolabelled products were characterised by analytical radio-HPLC. ^{89}Zr -labelled protein samples were characterised by manual SEC and automatic SEC-HPLC methods.

Quantification of radioactivity

Fractions obtained from manual SEC and tissues collected from the animal experiments were measured on a gamma counter (HIDEX Automatic Gamma Counter, Hidex AMG, Turku, Finland) by using a counting time of 30 s, and an energy window between 480–558 keV for ^{89}Zr (511 keV emission). Appropriate background and decay corrections were applied throughout.

Activity measurements were performed by using a dose calibrator (ISOMED 2010 Activimeter, Nuklear-Medizintechnik Dresden GmbH, Germany).

The radiochemical purity (RCP) of labelled protein samples was determined by automated SEC-HPLC (see above).

Photochemistry

Photochemical conjugation experiments were performed in transparent glass vials using an ultra-violet light-emitting diode (LED; 395 nm). The LED intensity was adjusted by using a digital UV-LED controller (Opsytec Dr. Gröbel GmbH, Ettlingen, Germany), where 100% corresponded to a power of approximately 355 mW at 395 nm. LED intensity was measured by using a S470C Thermal Power Sensor Head Volume Absorber, 0.25–10.6 μm , 0.1 mW–5W, $\varnothing 15$ mm. The LED (395 nm) had a maximum emission intensity at 389.9 nm (full-width-half-maximum of 9.1 nm). Photochemical reactions were stirred gently (stirring rate <100 rpm) to avoid potential mechanical damage to the protein. The temperature of all photochemical conjugation reactions was 23 ± 2 °C.

Cell culture

The human gastric cancer cell line MKN-45 was obtained from the Leibniz Institute DSMZ-German collection of Microorganisms and Cell Cultures (ACC 409). Cells were cultured at 37 °C in a humidified 5% CO_2 atmosphere in RPMI-1640 media (without phenol-red) supplemented with fetal bovine serum (FBS, 10% v/v, ThermoFisher Scientific) and penicillin/streptomycin (P/S, 1% v/v of penicillin 10000

U/mL and streptomycin 10 mg mL⁻¹). Cells were grown by serial passage and were harvested using trypsin-EDTA solution (0.025%).

Immunoreactivity (Lindmo-type cell binding assay)

Immunoreactivity was determined by using a procedure adapted from Lindmo and co-workers.¹ Cells were harvested and a series of six concentrations of 1:2 dilutions (in triplicate) was prepared in appropriate cell media. The purified radiotracer was added to each cell concentration in stated quantities. To determine the extent of non-specific binding, a fourth concentration series of the highest three concentrations was prepared and a specified quantity of non-radiolabelled sample was added to the cell suspension 30 min before the addition of the radiotracer. Three samples of the same specified quantity of radiotracer were also prepared to serve as standards for total activity added to each sample. Cells were shaken at 800 rpm at 37 °C in a thermomixer. Cell assays were incubated for 4 h. The cells were pelleted by centrifugation (2000 rpm, 4 °C, 4 min), the media was discarded, and the pellet was washed twice with ice cold PBS (2 × 1 mL) with re-pelleting and removal of PBS between each wash. Cell-associated radioactivity of the washed pellet was measured with use of the gamma counter. The immunoreactive fraction was determined by fitting the saturation binding curve and reciprocal Lindmo-plot by using the GraphPad Prism software.

Animals and xenograft models

All experiments involving mice were conducted in accordance with an animal experimentation license approved by the Zurich Canton Veterinary Office, Switzerland (Jason P. Holland). Experimental procedures planned and conducted in accordance with the ARRIVE 2.0 guidelines. Male or female athymic nude mice (CrI:NU(NCr)-*Foxn1*^{nu}, 20–31 g, 6–8 weeks old) were obtained from Charles River Laboratories Inc. (Freiburg im Breisgau, Germany), and were allowed to acclimatise at the University of Zurich Laboratory Animal Services Centre vivarium for 1 week prior to experimentation. Mice were provided with food and water *ad libitum*. Tumours were induced on the right shoulder or flank by subcutaneous (s.c.) injection of 2.5×10^6 MKN-45 cells. The cells were injected in a 150–200 µL suspension of a 1:1 v/v mixture of sterile PBS (pH7.4) and reconstituted basement membrane (Corning® Matrigel® Basement Membrane Matrix, obtained from VWR International). Tumours developed after a period of 10 days and the average volume of the MKN-45 tumours was 229 ± 127 mm³ ($n = 10$ mice). Mice were randomised before the study.

Small-animal positron emission tomography (PET) imaging

PET imaging experiments were conducted on a Genesis G4 PET/X-ray scanner (Sofie Biosciences, Culver City, CA). Approximately 3 min prior to recording each PET image, mice were anaesthetised by inhalation of between 2–4% isoflurane (Attane™, Piramal Enterprises Ltd, India, supplied by Provet AG, Lyssach, Switzerland)/oxygen gas mixture and placed on the scanner bed in the prone position. PET

images were recorded at various timepoints between 0–72 h post-administration of the radiotracer. anaesthesia was maintained by an experience animal experimenter by controlling the isoflurane dose between 1.5–2.0%. List-mode data were acquired for 15 min by using a γ -ray energy window of 150–650 keV, and a coincidence timing window of 20 ns. Images were reconstructed by iterative ordered subset maximum expectation (OSEM; 60 iterations) protocols. The reported reconstructed spatial resolution is 2.4 μ L at the centre of the field-of-view. Image data were normalised to correct for non-uniformity of response of the PET, attenuation, random events, dead-time count losses, positron branching ratio, and physical decay to the time of injection, but no scatter or partial-volume averaging correction was applied.

PET image quantification by volume-of-interest (VOI) analysis

An empirically determined system calibration factor (in units of [Bq/voxel]/[MBq g⁻¹] or [Bq cm⁻³]/[MBq g⁻¹]) for mice was used to convert voxel count rates to activity concentrations. The resulting image data were normalised to the administered activity to parameterise images in terms of %ID/cm³ (equivalent to units of %ID g⁻¹ assuming a tissue density of unity). Images were analysed by using VivoQuant™ 3.5 patch 2 software (InviCRO, Boston, MA). For image quantification, 3-dimensional volumes-of-interest were drawn manually to determine the radioactivity accumulation (decay corrected to the time of injection in units of %ID cm⁻³) in various tissues.

Biodistribution studies (ex vivo)

Biodistribution studies were conducted after the final imaging time point to evaluate the radiotracer uptake in tumour-bearing mice. Animals ($n = 5$ mice per group) were anaesthetised individually by isoflurane and euthanised by isoflurane asphyxiation followed by terminal exsanguination. A total of 15 tissues (including the tumour) were removed, rinsed in water, dried in air for approx. 2 min., weighed and counted on a calibrated gamma counter for accumulation of activity. The mass of radiotracer formulation injected into each animal was measured and used to determine the total number of counts per minute (cpm) injected into each mouse by comparison to a standard syringe of known activity and mass. Count data were background- and decay-corrected, and the tissue uptake for each sample (determined in units of percentage injected dose per gram [%ID g⁻¹]) was calculated by normalisation to the total amount of activity injected for each individual animal.

Effective half-life measurements

The effective half-life $t_{1/2}(\text{eff})$ / h was calculated from the measurement of total internal radioactivity, in mouse models, over time by using a dose calibrator.

Statistical analysis

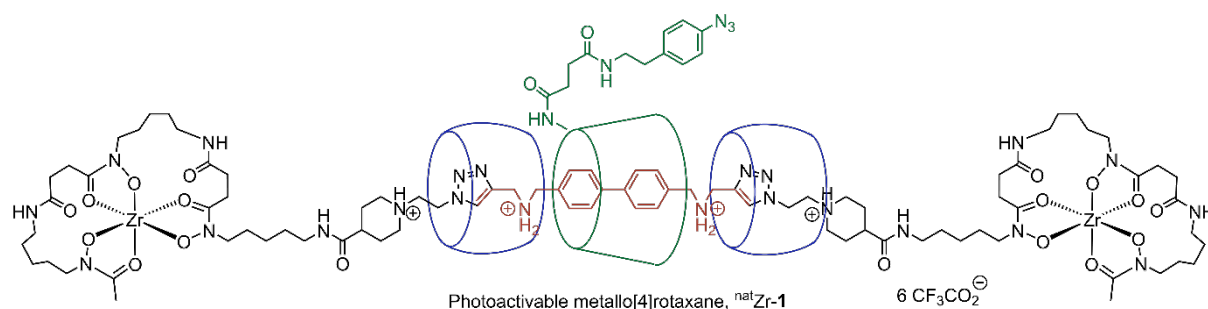
Where appropriate, data were analysed by the unpaired, two-tailed Student's *t*-test. Differences at the 95% confidence level, (*) *P*-value <0.05, were considered statistically significant. Note: (**) *P*-value <0.01; (***) *P*-value <0.001.

Synthesis and Characterisation

The aryl azide monofunctionalised β -CD, the biphenyl-dialkyne guest molecule, the desferrioxamine B-azido chelate and cucurbit[6]uril were synthesised following procedures described elsewhere.²

Metallo[4]rotaxane ^{nat}Zr-1

See also main text Scheme 1



Synthesis of ^{nat}Zr-1 was reported elsewhere.³ Briefly, to a suspension of compound **1** containing a desmetallated DFO chelate in H₂O (5 mL), a solution of ZrCl₄ (2 equiv.) in H₂O (0.5 mL) was added dropwise. The resulting clear, colourless solution was stirred at 23 °C for 2 h. After evaporation of the solvent under reduced pressure, the crude mixture was purified by semi-preparative HPLC using the method previously described. After lyophilisation, the ^{nat}Zr complexes were obtained as slightly yellow residue. The product was estimated by analytical HPLC to have a purity >95%; HRMS (ESI) *m/z* calcd for C₂₁₂H₂₉₂DN₇₅O₇₈Zr₂ [M+4H]⁴⁺ 886.3234 found 886.3198 (100%).

Radiosynthesis of [^{89}Zr]Zr-1

Radiolabelling reactions to prepare [^{89}Zr]Zr-1 were accomplished by the addition of an aliquot of neutralized [^{89}Zr][Zr(C₂O₄)₄]⁴⁻ stock solution (~7 MBq) to an aqueous solution of **1** (36 μL of 1 mg mL⁻¹ stock in H₂O) with a total reaction volume of 130 μL . The reactions were monitored by radio-iTLC (50 mM aqueous DTPA at pH 7.4) and complexation was found to be complete in less than 10 min at 23 °C giving a radiochemical conversion (RCC) >99% ($R_f = 0.0 - 0.1$). The product was characterized by analytical HPLC following the method described in the general section. Note: the UV-Vis detector and radioactivity detector were arranged serially with an offset time of approximately 0.10-0.30 min (depending on temperature). The identity of the radiolabelled compound ([^{89}Zr]Zr-1) was confirmed by co-injection with an authenticated sample of non-radiolabelled complex ^{nat}Zr-1.

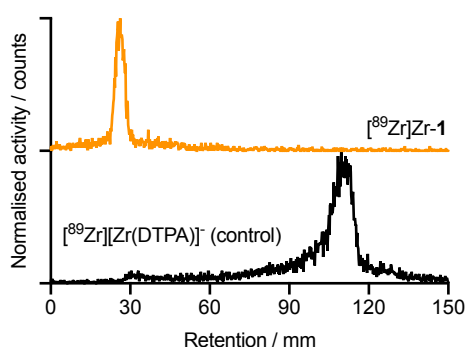
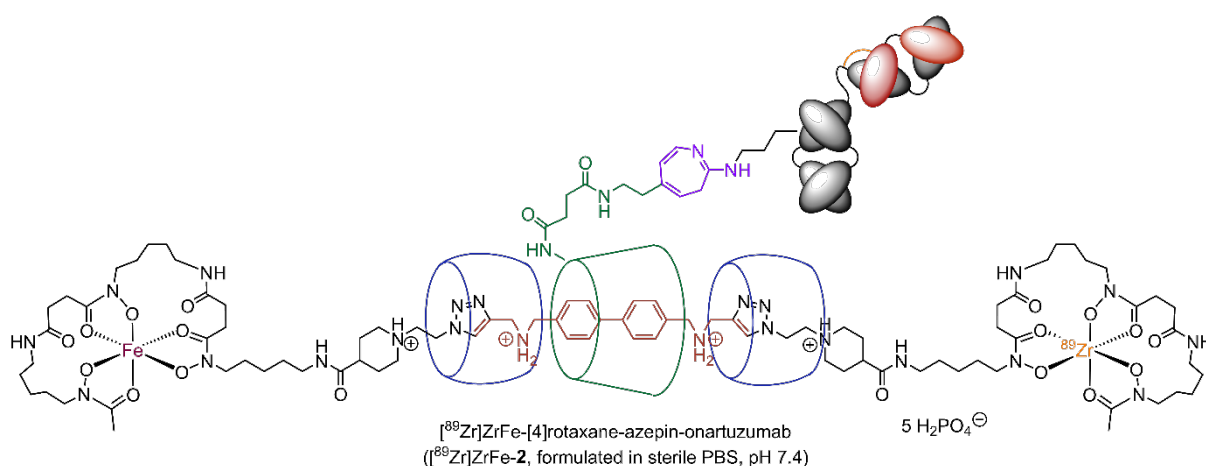


Figure S1. Radio-TLC chromatograms for [^{89}Zr]Zr-1 (orange) in 50 mM DTPA and the associated control sample, [^{89}Zr][Zr(DTPA)]⁻.

Photoradiosynthesis of [^{89}Zr]ZrFe-[4]rotaxane-azepin-onartuzumab, [^{89}Zr]ZrFe-2

Simultaneous, one-pot photochemical conjugation and ^{89}Zr -radiolabelling reactions were performed in accordance with the following general procedure. Compound **1**, (MW = 5270.9 g mol $^{-1}$, 36 μL , 0.38 mM H $_2\text{O}$ solution, 72 μg , 13.66 nmol), neutralised [^{89}Zr][Zr(C $_2\text{O}_4$) $_4$] $^{4-}$ (8.73 MBq, 12 μL , pH8.3), Chelex water (90 μL) were stirred gently at 23 $^\circ\text{C}$ for 1 minute. After radio-iTLC check to ensure quantitative radiochemical conversion and control pH8–8.5, onartuzumab (60.0 mg mL $^{-1}$, MW = 99180 g mol $^{-1}$, PBS pH7.4, 12 μL , 0.72 mg, 7.26 nmol, photoactivable compound-to-mAb ratio was 1.9 to 1) was added at 23 $^\circ\text{C}$ (total volume reaction 150 μL , pH8.3). The reaction mixture was gently stirred and irradiated at 100% LED intensity for 15 min at 395 nm. After the irradiation, reactions were then quenched by the addition of FeCl $_3$ (2 equiv. with respect to compound **1**, 28 nmol, 1 minute, corresponding to a 1:1 ratio between Fe $^{3+}$ ions and the total number of DFO ligands used), then DTPA (50 mM, 10 μL , 500 nmol, pH7, 1 minute). Aliquots of the crude reaction mixtures were retained for analysis. The remaining material was purified by preparative Sephadex G-100 SEC (collecting the 1.4–3.0 mL high molecular weight fraction using sterile PBS as an eluent). The combined fractions were transferred to a 10 kDa Millipore spin filtration falcon tube (5 mL) and concentrated at 4000 rpm for 15 min at 23 $^\circ\text{C}$. Crude and purified aliquots were analysed by using analytical radio-iTLC, Sephadex G-100 SEC, and SEC-HPLC.



Scaled-up photoradiosynthesis of [^{89}Zr]ZrFe-[4]rotaxane-azepin-onartuzumab for biological experiments

The one-pot simultaneous ^{89}Zr -radiolabelling and photochemically induced functionalisation to produce [^{89}Zr]ZrFe-[4]rotaxane-onartuzumab was scaled-up to obtain sufficient material for the biological studies in cells and animals.

To a glass vial containing H $_2\text{O}$ (44 μL ; Chelex treated 18.2 M $\Omega\cdot\text{cm}$), the [4]pseudorotaxane **1** stock solution (36 μL , 0.38 mM, 13.66 nmol) and an aliquot of the neutralised stock solution of [^{89}Zr][Zr(C $_2\text{O}_4$) $_4$] $^{4-}$ (20 μL , 13.17 MBq, pH 8.0) was added an aliquot of the stock solution of onartuzumab was added (prepurified, stock concentration = 60.0 mg/mL, MW(onartuzumab) = 99,180 Da, volume added = 12 μL , protein mass = 0.72 mg, protein moles = 7.26 nmol). The initial chelate-to-mAb ratio

was 2 to 1. The reaction pH was measured and was between 8.1 – 8.3. The total reaction volume was ~150 μL giving a final $[\text{mAb}] = 48.4 \mu\text{M}$, and a final $[1] = 90.3 \mu\text{M}$. The reaction was stirred gently at 23 $^{\circ}\text{C}$ and irradiated directly from the top of the vial for 15 min. After the irradiation, reactions were then quenched by the addition of $\text{FeCl}_3 \cdot \text{H}_2\text{O}$ (3.5 μL , 8 mM, 28 nmol), DTPA (10 μL , 50 mM, pH7) and aliquots of the crude reaction mixtures were purified by preparative Sephadex G-100 SK-10-SEC (collecting the 2.0 – 3.4 mL high molecular weight fraction using sterile PBS as an eluent). The combined fractions were transferred to a 10 kDa Millipore spin filtration falcon (5 mL) and concentrated at 4000 rpm for 15 min at 23 $^{\circ}\text{C}$. Crude and purified aliquots were analysed by using analytical radio-iTLC, Sephadex G-100 SK-10-SEC and SEC-HPLC. The isolated decay corrected radiochemical yield (RCY) of ^{89}Zr ZrFe-[4]rotaxane-onartuzumab was 10.8% ($n = 1$) and the lower limit of the molar activity of the product (estimated by assuming no protein losses) was $\sim 0.61 \text{ MBq nmol}^{-1}$ of protein, with an activity concentration of 9.88 MBq mL^{-1} . The radiochemical purity of the purified samples of ^{89}Zr ZrFe-[4]rotaxane-onartuzumab was estimated to be $\sim 90\%$ (measured by SEC-HPLC).

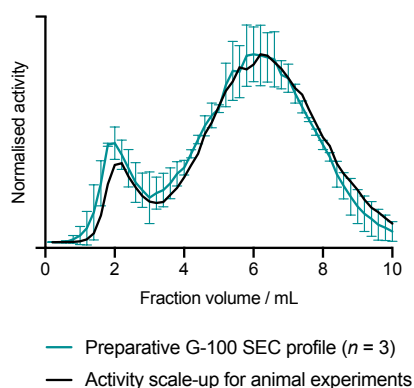


Figure S2. Preparative Sephadex G100-SEC profiles for the purification of ^{89}Zr ZrFe-[4]rotaxane-azepin-onartuzumab ($n = 3$, green) and with a scale-up of the activity for animal experiments (black).

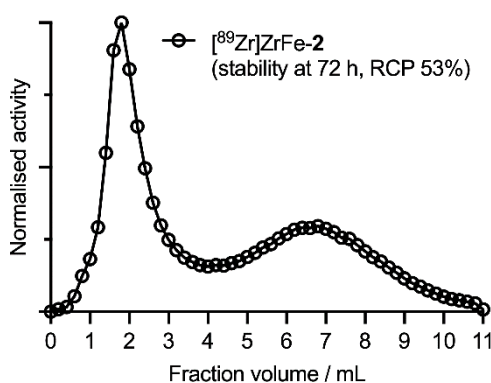


Figure S3. Size-exclusion (G100) chromatogram of ^{89}Zr ZrFe-2 after incubation in the formulation buffer for 72 h at ambient conditions.

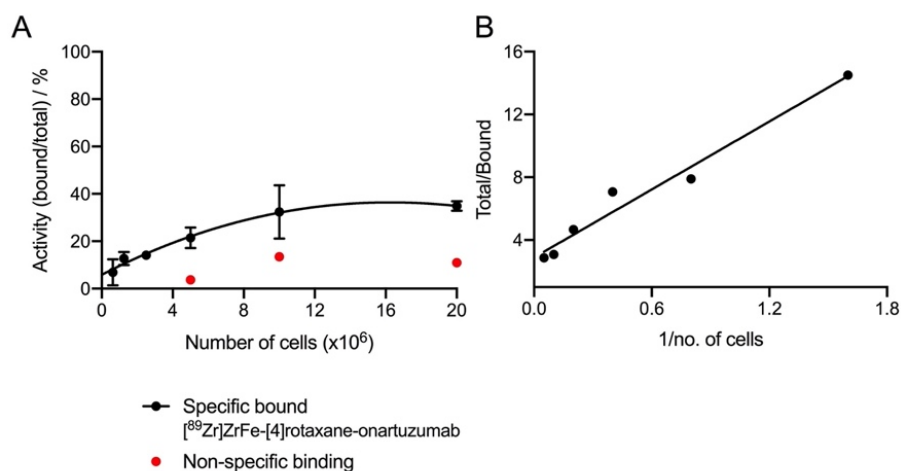


Figure S4. Cellular binding (Lindmo) assay on $[^{89}\text{Zr}]\text{ZrFe-[4]rotaxane-azepin-onartuzumab}$.

(a) Saturation binding curve of $[^{89}\text{Zr}]\text{ZrFe-[4]rotaxane-onartuzumab}$, $[^{89}\text{Zr}]\text{ZrFe-2}$, on an increasing number of MKN-45 cells, and (b) a plot showing the classic Lindmo transformation of the cell binding data which can be used to estimate the immunoreactivity of the radiotracer from the determination of the value of 1/y-intercept.

Animal studies and preparation of $[^{89}\text{Zr}]\text{ZrFe-[4]rotaxane-azepin-onartuzumab}$ doses for injection in mice

An aliquot of the purified and formulated sample of $[^{89}\text{Zr}]\text{ZrFe-[4]rotaxane-azepin-onartuzumab}$ ($[^{89}\text{Zr}]\text{ZrFe-2}$, 170 μL , 1.630 MBq) was added to a sterile vial and diluted with sterile PBS to a final volume of 1.8 mL. The tail of each mouse was warmed gently by using a warm water bath ($\sim 30^\circ\text{C}$) immediately before administering $[^{89}\text{Zr}]\text{ZrFe-[4]rotaxane-azepin-onartuzumab}$. Two groups of animals were used whereby each mouse in the normal group ($n = 5$ mice) received a dose containing 0.192–0.198 MBq of activity (31–32 μg of protein, in 200 μL sterile PBS) *via* intravenous (i.v.) tail-vein injection ($t = 0$ h). For the competitive inhibition (blocking) experiments, a separate aliquot of $[^{89}\text{Zr}]\text{ZrFe-2}$ (150 μL , 1.449 MBq) was added to a sterile vial. Then an aliquot of the stock solution of MetMAb (fully formulated; 60.0 mg mL^{-1} , 115 μL , 6.9 mg of protein) was added to reduce the molar activity (total ~ 1.02 mg of protein/mouse) and the mixture was diluted with sterile PBS to a final volume of 1.4 mL. Animals in the blocking group ($n = 5$ mice) each received an i.v. dose containing 0.219–0.229 MBq (in 200 μL sterile PBS).

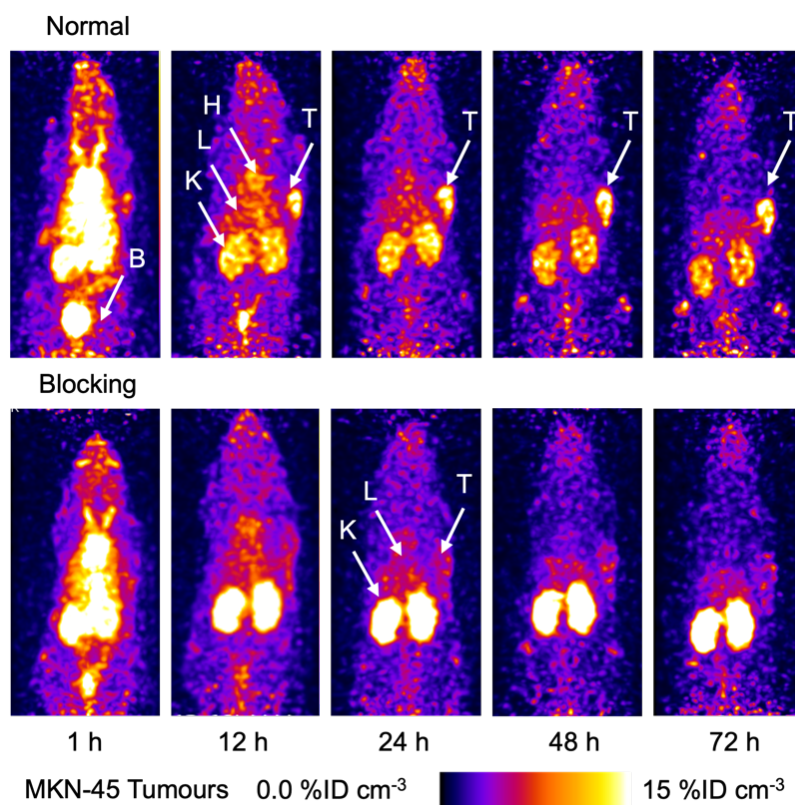


Figure S5. Maximum intensity project (MIP) ^{89}Zr ZrFe-2 PET images of a representative mouse from the normal (top) and blocking (bottom) group.

Images were recorded between 1 – 72 h post-administration). T = tumour, H = heart, L = liver, B = bladder, K = kidney.

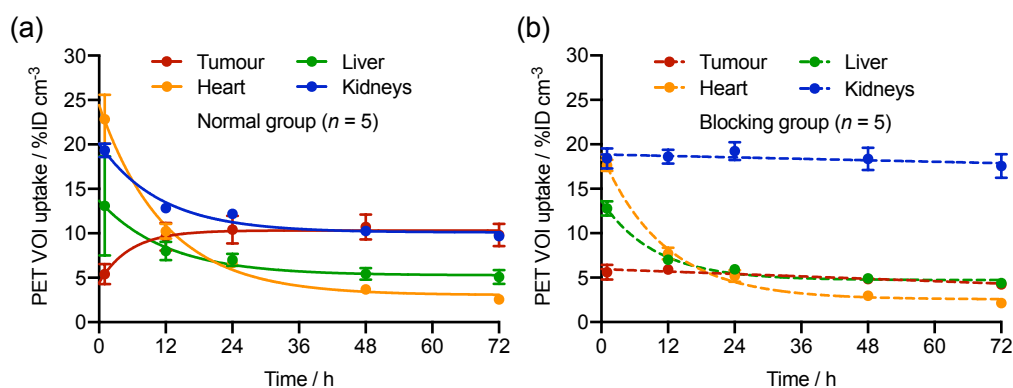


Figure S6. Time-activity curves (TACs) obtained from quantitative volume-of-interest (VOI) analysis from the normal ($n = 5$), and (g) the blocking ($n = 5$) group of animals illustrating the tumour specificity of [⁸⁹Zr]ZrFe-2.

Table S1. Quantitative data from the VOI analysis of the PET images.

Time / h	Tissue VOI activity (%ID cm ⁻³) versus time					
	[⁸⁹ Zr]ZrFe-[4]rotaxane-azepin-onartuzumab, [⁸⁹ Zr]ZrFe-2					
	Tumour	Heart	Liver	Brain	Muscle	Kidney
Normal group ($n = 5$)						
1	5.41 ± 1.13	22.84 ± 2.74	13.10 ± 5.56	2.51 ± 0.58	2.15 ± 0.37	19.34 ± 0.76
12	9.60 ± 1.57	10.24 ± 0.82	8.01 ± 1.04	1.59 ± 0.17	1.83 ± 0.33	12.83 ± 0.56
24	10.40 ± 1.54	6.65 ± 0.38	7.01 ± 0.69	1.37 ± 0.17	1.45 ± 0.51	12.18 ± 0.48
48	10.71 ± 1.41	3.68 ± 0.42	5.45 ± 0.66	1.26 ± 0.28	0.95 ± 0.28	10.25 ± 0.38
72	9.80 ± 1.26	2.56 ± 0.38	5.07 ± 0.77	1.09 ± 0.12	0.70 ± 0.16	9.70 ± 0.35
Blocking group ($n = 5$)						
1	5.60 ± 0.84	17.63 ± 0.63	12.80 ± 0.82	2.32 ± 0.35	1.90 ± 0.44	18.40 ± 1.12
12	5.91 ± 0.45	7.71 ± 0.65	7.00 ± 0.47	1.62 ± 0.33	1.46 ± 0.44	18.60 ± 0.79
24	5.65 ± 0.42	5.18 ± 0.65	5.93 ± 0.52	1.06 ± 0.09	1.26 ± 0.13	19.24 ± 0.99
48	4.84 ± 0.38	2.96 ± 0.27	4.92 ± 0.37	1.01 ± 0.22	0.76 ± 0.28	18.35 ± 1.25
72	4.25 ± 0.33	2.15 ± 0.15	4.38 ± 0.45	0.90 ± 0.16	0.72 ± 0.17	17.57 ± 1.33

Biodistribution results

Table S2. *Ex vivo* biodistribution data measured at 72 h after i.v. administration of [⁸⁹Zr]ZrFe-[4]rotaxane-azepin-onartuzumab (normal and blocking groups) in female athymic nude mice bearing subcutaneous MKN-45 tumours.

Tissue	[⁸⁹ Zr]ZrFe-[4]rotaxane-azepin-onartuzumab, [⁸⁹ Zr]ZrFe-2 (Normal group, <i>n</i> = 5)		[⁸⁹ Zr]ZrFe-[4]rotaxane-azepin-onartuzumab, [⁸⁹ Zr]ZrFe-2 (Blocking group, <i>n</i> = 5)	
	Uptake / %ID g ⁻¹ ± S.D. ^[a]	Tumour-to-tissue contrast ratio ± S.D. ^[b]	Uptake / %ID g ⁻¹ ± S.D. ^[a]	Tumour-to-tissue contrast ratio ± S.D. ^[b]
Blood	1.38 ± 0.32	7.12 ± 0.45	0.99 ± 0.09	2.45 ± 0.51
Tumour	9.90 ± 2.84	1.00 ± 0.00	2.39 ± 0.29	1.00 ± 0.00
Heart	0.93 ± 0.41	12.11 ± 4.67	0.64 ± 0.12	3.81 ± 0.71
Lungs	2.79 ± 1.38	4.90 ± 3.49	0.94 ± 0.12	2.56 ± 0.31
Liver	3.23 ± 0.45	3.16 ± 1.19	2.77 ± 0.36	0.87 ± 0.12
Spleen	2.31 ± 0.43	4.33 ± 1.04	1.68 ± 0.38	1.48 ± 0.38
Stomach	0.22 ± 0.08	47.90 ± 14.04	0.17 ± 0.04	14.36 ± 2.13
Pancreas	0.28 ± 0.15	29.20 ± 4.80	0.25 ± 0.05	9.86 ± 2.77
Kidney	13.07 ± 1.54	0.76 ± 0.19	25.43 ± 3.01	0.10 ± 0.02
Sm. Int.	0.78 ± 1.00	24.02 ± 12.65	0.30 ± 0.03	7.90 ± 1.19
Large Int.	0.18 ± 0.02	54.94 ± 13.01	0.25 ± 0.05	9.69 ± 1.89
Fat	0.15 ± 0.04	62.02 ± 26.46	0.27 ± 0.07	9.23 ± 2.21
Muscle	0.31 ± 0.14	35.75 ± 11.02	0.20 ± 0.08	13.10 ± 4.24
Bone	2.32 ± 1.59	5.04 ± 2.85	1.06 ± 0.72	3.01 ± 1.68
Skin	0.75 ± 0.19	12.41 ± 4.57	0.99 ± 0.16	2.57 ± 0.33

^[a] Uptake data are expressed as the mean %ID g⁻¹ ± one standard deviation (S.D. / %ID g⁻¹).

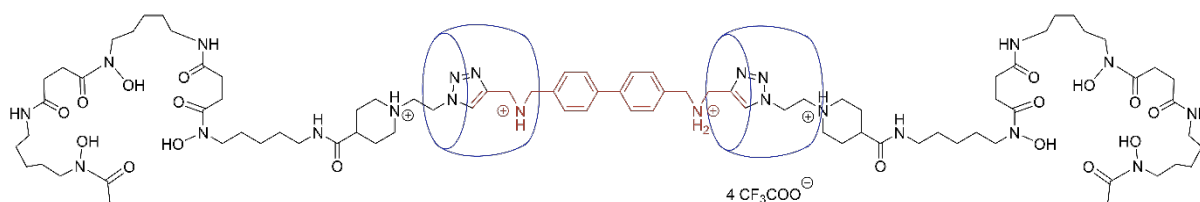
^[b] Errors for the tumour-to-tissue ratios are calculated as the standard deviations based on ratios from dependent pairs.

Preparation of [⁸⁹Zr]ZrFe-[4]rotaxane-2-hydroxyazepin [⁸⁹Zr]ZrFe-3

As previously described,³ [⁸⁹Zr]ZrFe-[4]rotaxane-2-hydroxyazepin ([⁸⁹Zr]ZrFe-3) is likely the major small-molecule byproduct produced and isolated after irradiation of [⁸⁹Zr]ZrFe-[4]rotaxane-mAb.

An aliquot of the small-molecule fractions obtained during the purification of [⁸⁹Zr]ZrFe-[4]rotaxane-mAb (400 µL, 2.602 MBq) was added to a sterile vial and diluted with sterile PBS to a final volume of 0.9 mL.

Preparation of compound **4**



To a solution of the biphenyl-dialkyne (0.5 mg, 1.3 μmol , 1 equiv.) in H_2O (2 mL) were added CB[6] (2.6 mg, 2.6 μmol , 2 equiv.) and the desferrioxamine B-azido chelate (1.9 mg, 2.6 μmol , 2 equiv.). The resulting mixture was stirred at 50 $^\circ\text{C}$ for 12 h. The crude was purified using preparative HPLC at a flow rate of 7 mL min^{-1} with a linear gradient of A (MeOH, Sigma-Aldrich, HPLC grade) and B (distilled water containing 0.1% TFA): $t = 0$ min A 5% + B 95%, $t = 60$ min A 100% + B 0%. After lyophilisation, **4** was obtained as a white powder (3.1 mg, 64% yield); ^1H NMR (500 MHz, D_2O) $\delta = 7.97$ (d, $J = 7.9$ Hz, 2H), 7.92 (d, $J = 8.0$ Hz, 2H), 6.57 (s, 2H), 5.74 (dd, $J = 15.6, 29.6$ Hz, 24H), 5.52 (s, 24H), 4.55–4.64 (m, 4H), 4.41–4.48 (m, 4H), 4.37–4.41 (m, 4H), 4.28 (dd, $J = 13.1, 14.9$ Hz, 24H), 4.20 (t, $J = 7.1$ Hz, 4H), 3.92 (t, $J = 7.1$ Hz, 4H), 3.53–3.71 (m, 12H), 3.12–3.32 (m, 18H), 2.68–2.85 (m, 9H), 2.45–2.57 (m, 8H), 2.21–2.30 (m, 2H), 2.13 (s, 6H), 2.09–2.21 (m, 3H), 1.58–1.80 (m, 14H), 1.38–1.49 (m, 12H), 1.25–1.38 ppm (m, 12H); ^{13}C NMR (126 MHz, D_2O) $\delta = 176.0, 174.8, 173.8, 173.5, 162.9$ (q, $^2J = 35.6$ Hz), 156.5, 156.2, 140.9, 139.1, 131.3, 130.4, 127.3, 119.7, 116.3 (q, $^1J = 291.2$ Hz), 70.2, 52.8, 52.6, 51.4, 51.2, 47.8, 47.7, 44.5, 43.1, 40.0, 39.2, 30.5, 30.4, 27.9, 27.9, 27.6, 26.4, 25.4, 23.0, 19.2 ppm; HRMS (ESI) m/z calcd for $\text{C}_{158}\text{H}_{216}\text{N}_{70}\text{O}_{42}$ $[\text{M}+4\text{H}]^{4+}$ 941.4224 found 941.4209 (100%).

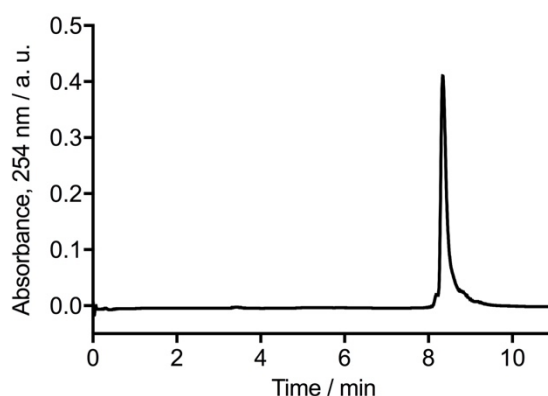


Figure S7. Reverse-phase analytical HPLC chromatogram of complex **4**, $\lambda = 254$ nm.

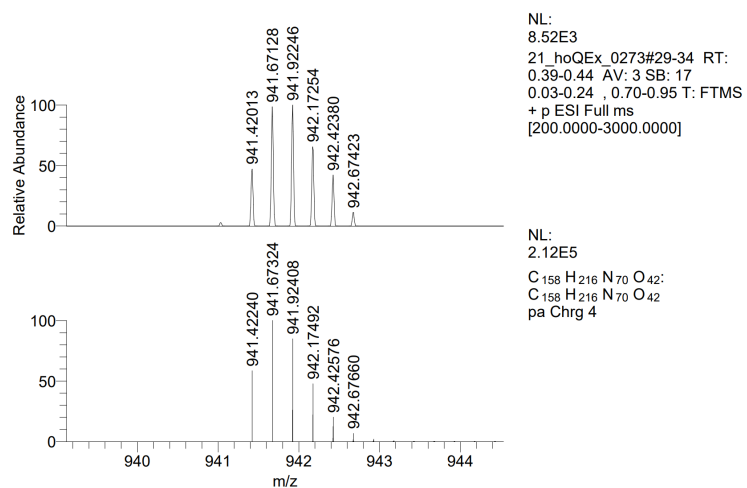


Figure S8. HRMS (ESI+) spectrum of compound **4**.

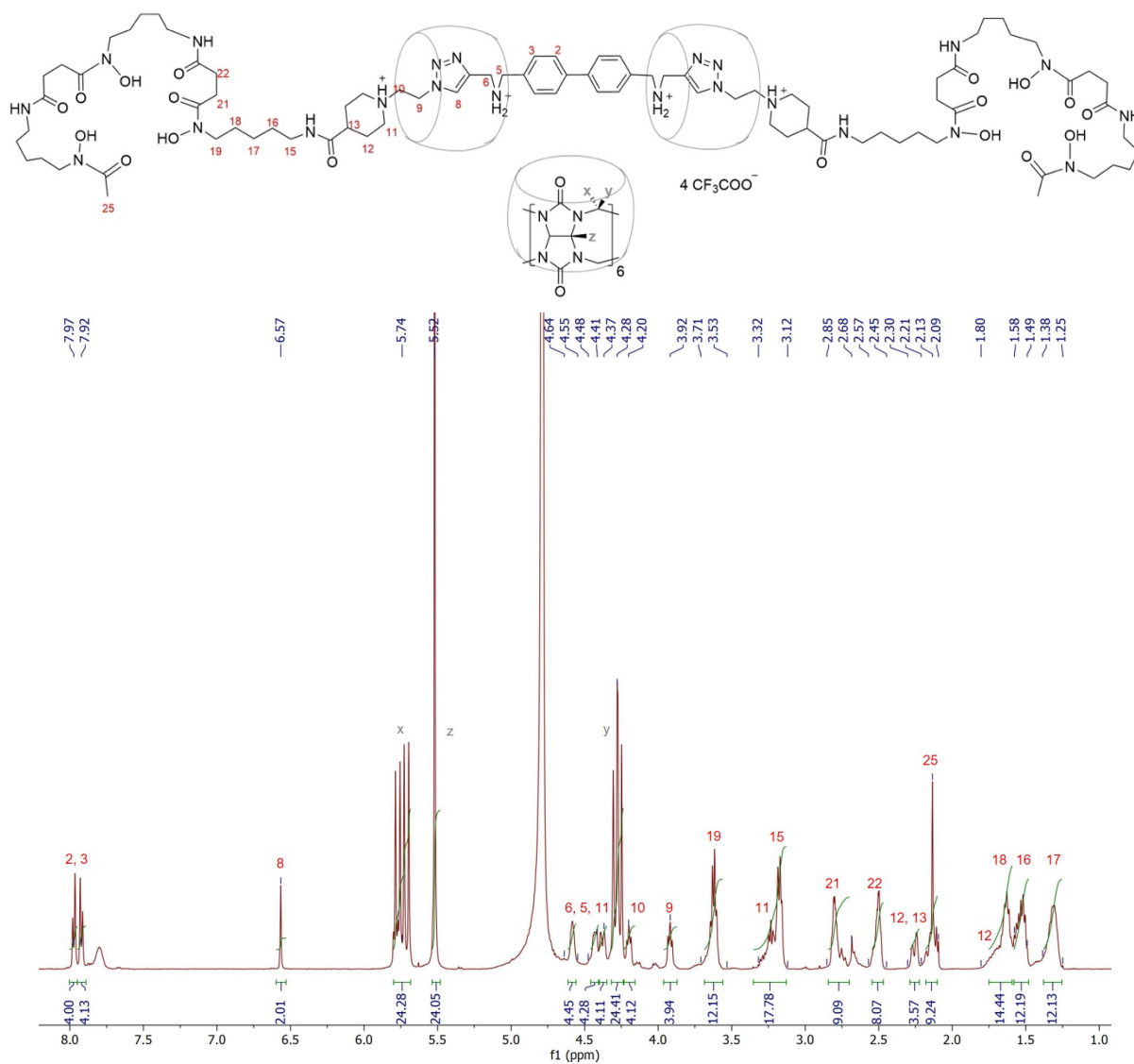


Figure S9. ¹H NMR of compound **4** (D₂O, 500 MHz).

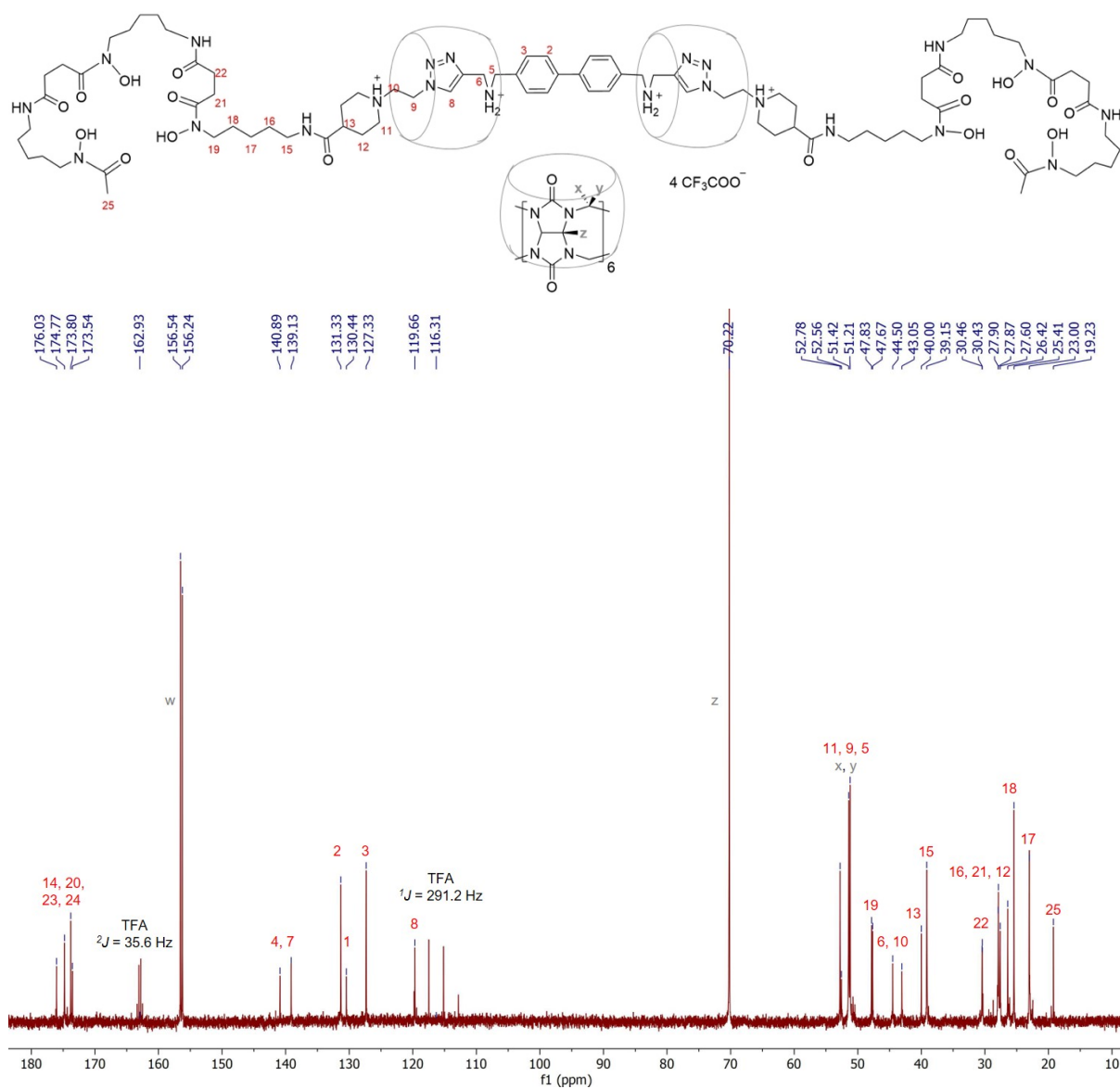


Figure S10. $^{13}\text{C}\{^1\text{H}\}$ NMR of compound 4 (D_2O , 126 MHz).

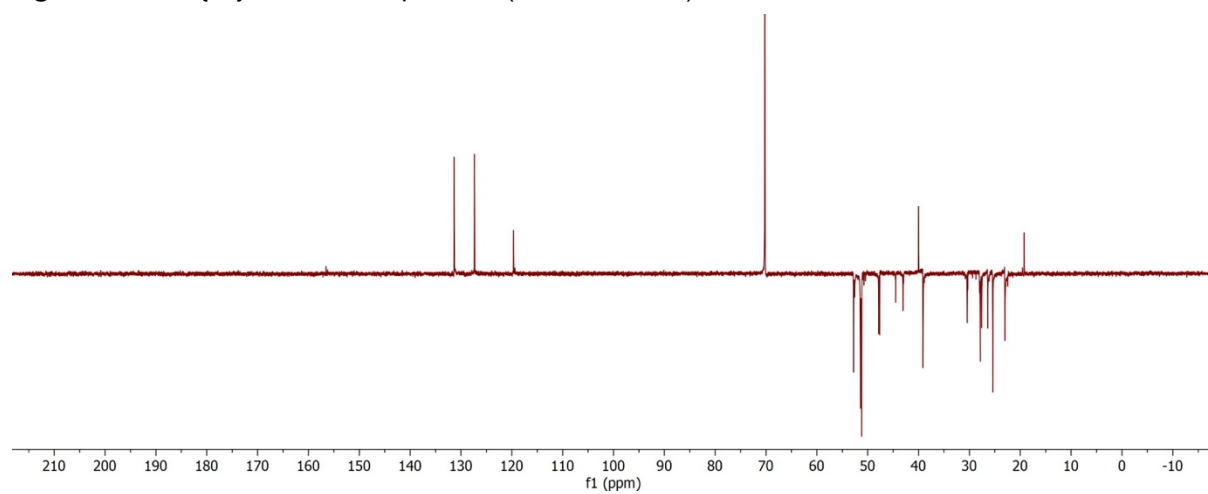


Figure S11. DEPT-135 of compound 4 (D_2O).

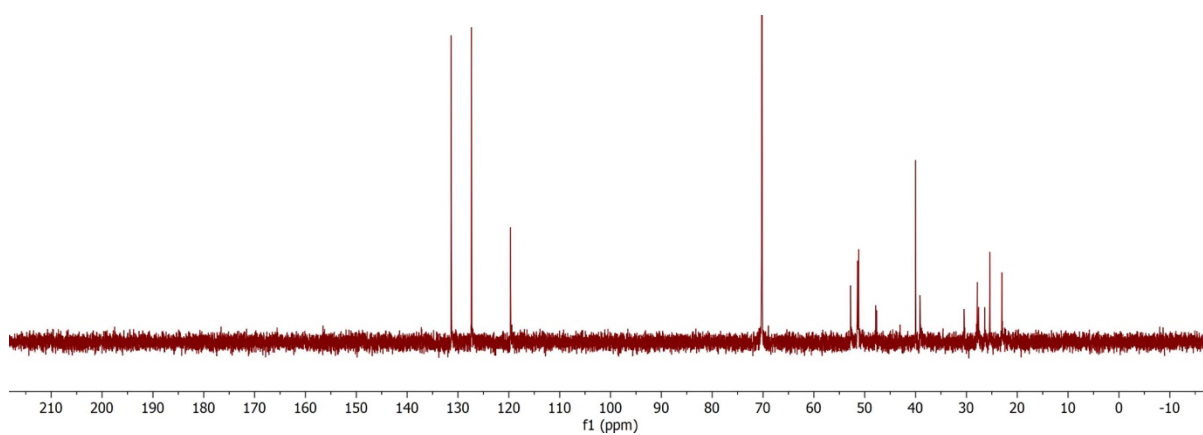


Figure S12. DEPT-90 of compound **4** (D₂O).

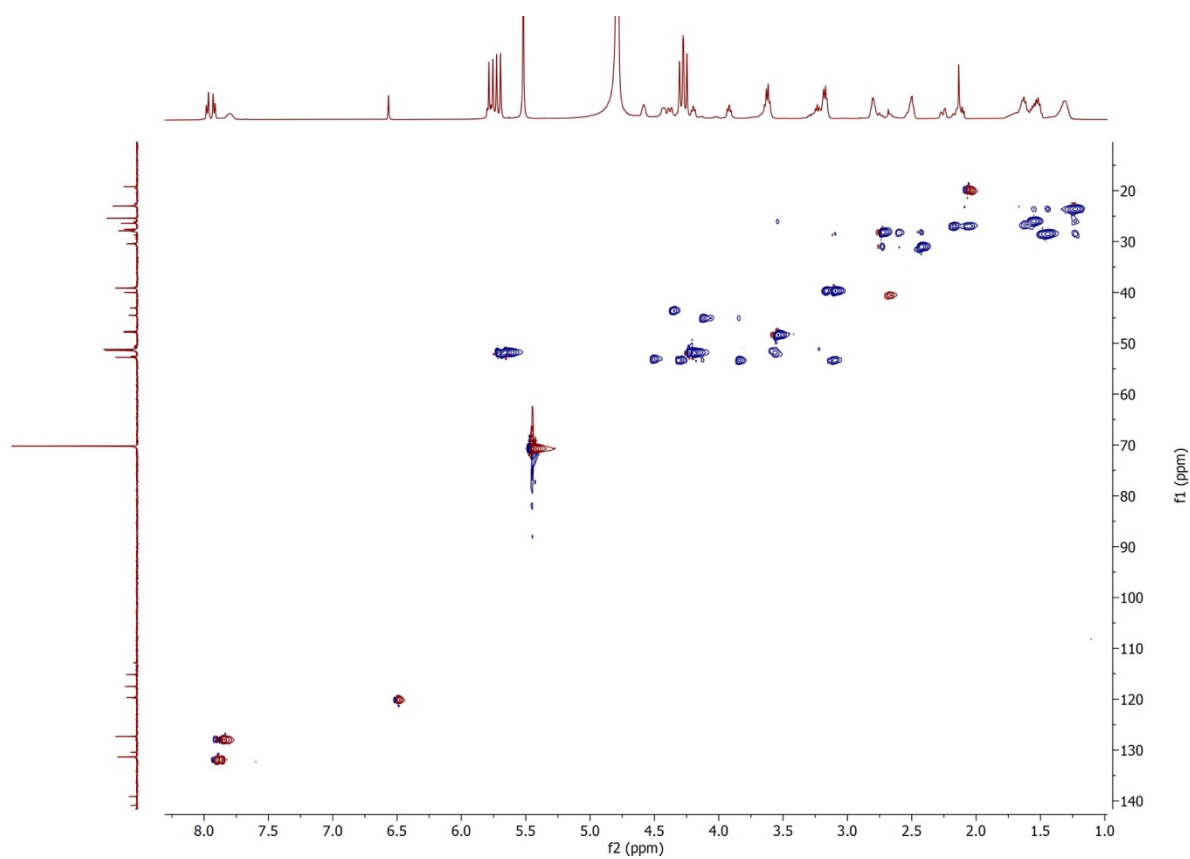


Figure S13. HSQC of compound **4** (D₂O).

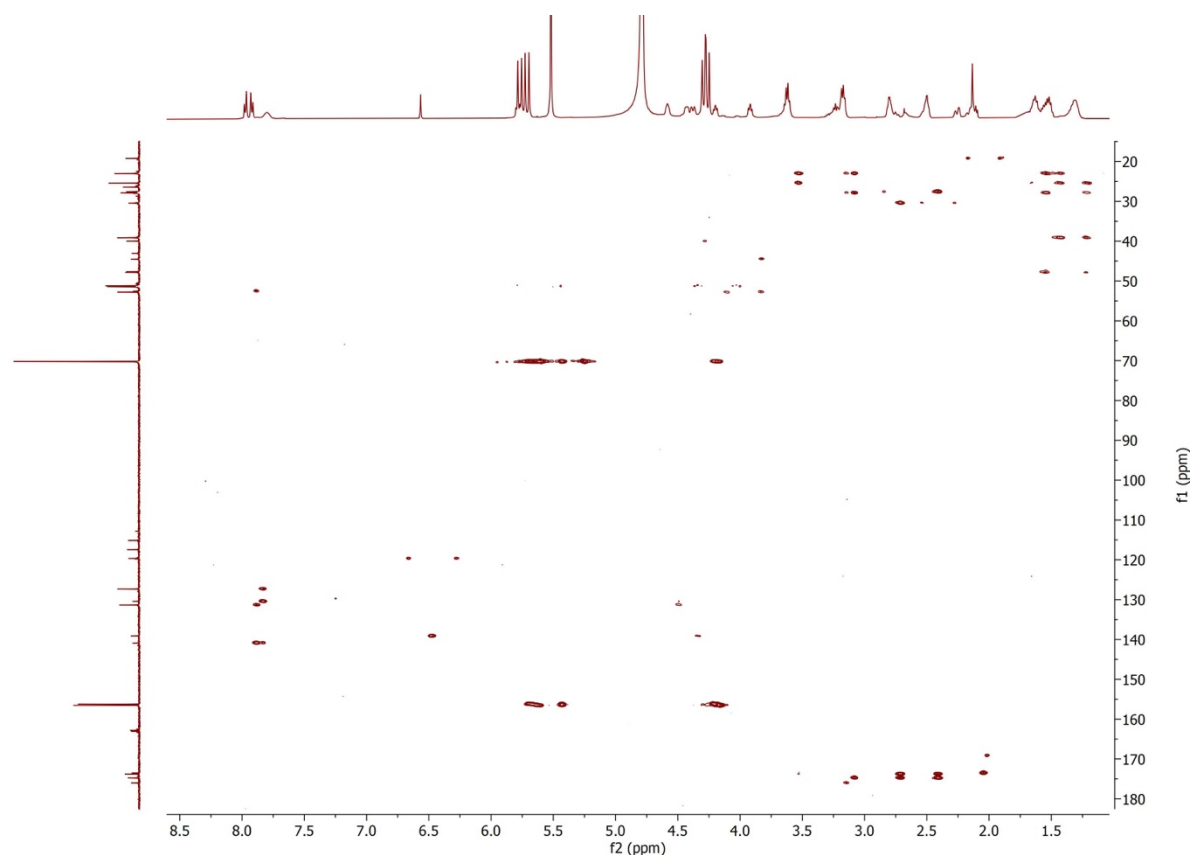
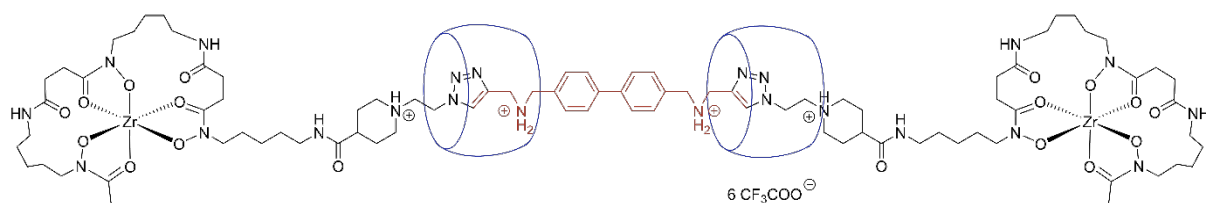


Figure S14. HMBC of compound **4** (D₂O).

Preparation of compound ^{nat}Zr-4



To a suspension of compound **4** containing a desmetallated DFO chelate in H₂O (5 mL), a solution of ZrCl₄ (2 equiv.) in H₂O (0.5 mL) was added dropwise. The resulting clear, colourless solution was stirred at 23 °C for 2 h. After evaporation of the solvent under reduced pressure, the crude mixture was purified by semi-preparative HPLC using the method previously described. After lyophilisation, the ^{nat}Zr complex was obtained as a slightly off-white residue. The product was estimated by analytical HPLC to have a purity >95%; HRMS (ESI) *m/z* calcd for C₁₅₈H₂₁₀N₇₀O₄₂Zr₂ [M+4H]⁶⁺ 656.5754 found 656.5743 (100%).

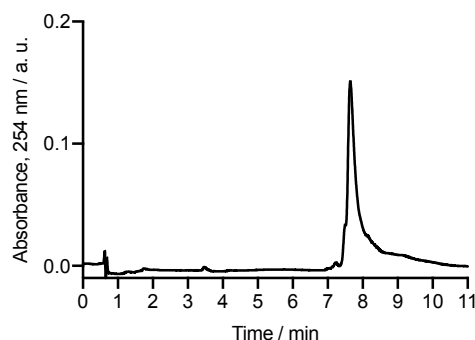


Figure S15. Reverse-phase analytical HPLC chromatogram of complex $^{nat}\text{Zr-4}$, $\lambda = 254$ nm.

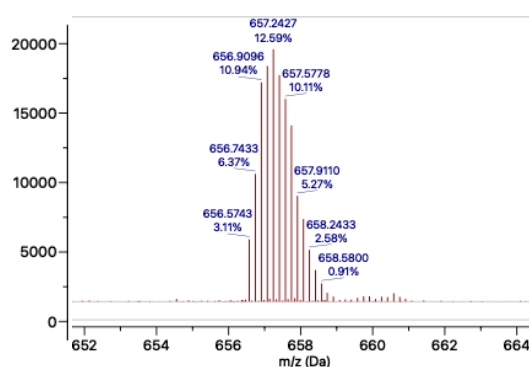


Figure S16. HRMS (ESI+) spectrum of compound $^{nat}\text{Zr-4}$.

Radiosynthesis of $[^{89}\text{Zr}]\text{ZrFe-4}$

Radiolabelling reactions to prepare $[^{89}\text{Zr}]\text{ZrFe-4}$ were accomplished by the addition of an aliquot of neutralized $[^{89}\text{Zr}][\text{Zr}(\text{C}_2\text{O}_4)_4]^{4-}$ stock solution (~ 3 MBq) to an aqueous solution of **4** (15 μL of 2 mg mL^{-1} stock) with a total reaction volume of 50 μL . FeCl_3 (1 μL of 2.2 mg mL^{-1} stock, 1 equiv.) was added to ensure rotaxane capping on both side of the axle. The reactions were monitored by radio-iTLC (50 mM aqueous DTPA at pH 7.4) and complexation was found to be complete in less than 10 min at 23 $^\circ\text{C}$ giving a radiochemical conversion (RCC) $>99\%$ ($R_f = 0.0 - 0.1$). The product was characterised by analytical HPLC following the method described in the general section. Note: the UV-Vis detector and radioactivity detector were arranged serially with an offset time of approximately 0.10-0.30 min (depending on temperature). The identity of the radiolabelled compound ($[^{89}\text{Zr}]\text{ZrFe-4}$) was confirmed by co-injection with an authenticated sample of non-radiolabelled complex $^{nat}\text{Zr-4}$.

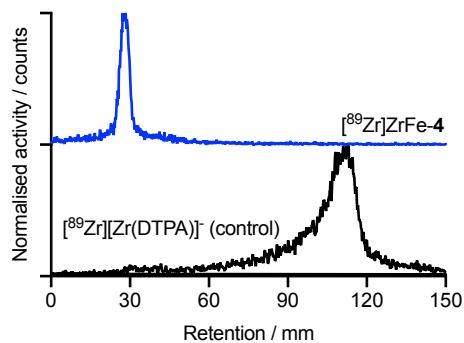


Figure S17. Radio-iTLC $[^{89}\text{Zr}]\text{ZrFe-4}$ (blue), and $[^{89}\text{Zr}]\text{Zr-DTPA}$ (black) as a control.

Effective half-life measurements

The effective half-life $t_{1/2}(\text{eff})$ of $[^{89}\text{Zr}]\text{ZrFe-3}$ and $[^{89}\text{Zr}]\text{ZrFe-4}$ was measured in female athymic nude mice. Total internal radioactivity was measured as a function of time by using a dose calibrator.

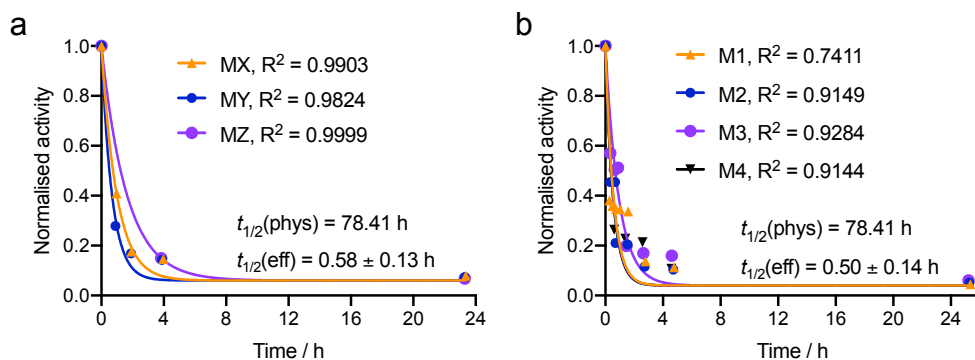


Figure S18. One-phase model for the experimentally measured effective half-life of (A) $[^{89}\text{Zr}]\text{ZrFe-3}$ ($n = 3$), and (B) $[^{89}\text{Zr}]\text{ZrFe-4}$ ($n = 4$).

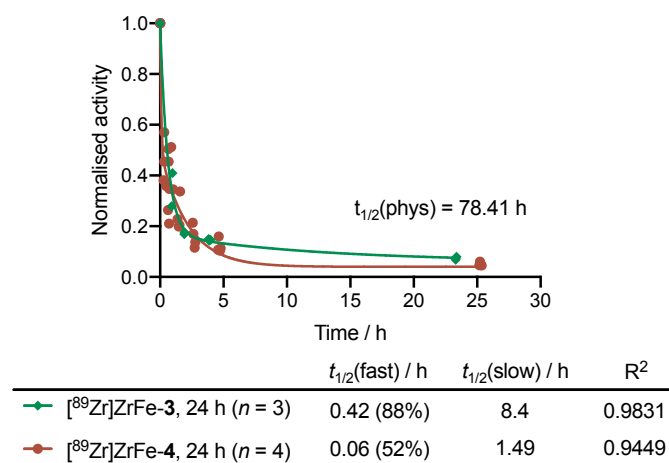


Figure S19. Two-phase excretion model for the experimentally measured effective half-life of $[^{89}\text{Zr}]\text{ZrFe-3}$ (green) and $[^{89}\text{Zr}]\text{ZrFe-4}$ (red).

Biodistribution results

Table S3. *Ex vivo* biodistribution data measured at 24 h after i.v. administration of $[^{89}\text{Zr}]\text{ZrFe-3}$ and $[^{89}\text{Zr}]\text{ZrFe-4}$ in female athymic nude mice.

Tissue	$[^{89}\text{Zr}]\text{ZrFe-3}$ ($n = 3$)	$[^{89}\text{Zr}]\text{ZrFe-4}$ ($n = 4$)
	Uptake / %ID $\text{g}^{-1} \pm \text{S.D.}^{[a]}$	Uptake / %ID $\text{g}^{-1} \pm \text{S.D.}^{[a]}$
Blood	0.11 ± 0.04	0.06 ± 0.02
Heart	0.14 ± 0.08	0.22 ± 0.05
Lungs	0.22 ± 0.09	0.74 ± 0.24
Liver	2.79 ± 0.18	2.92 ± 0.35
Spleen	0.41 ± 0.04	0.82 ± 0.23
Stomach	0.13 ± 0.01	0.16 ± 0.09
Pancreas	0.10 ± 0.06	0.14 ± 0.02
Kidney	12.00 ± 2.49	5.37 ± 1.41
Sm. Int.	0.11 ± 0.03	0.17 ± 0.02
Large Int.	0.23 ± 0.13	0.17 ± 0.04
Fat	0.26 ± 0.26	0.13 ± 0.05
Muscle	0.06 ± 0.04	0.12 ± 0.04
Bone	0.11 ± 0.01	0.5 ± 0.37
Skin	0.46 ± 0.47	0.7 ± 0.21

^[a] Uptake data are expressed as the mean %ID $\text{g}^{-1} \pm$ one standard deviation (S.D. / %ID g^{-1}).

References

1. Konishi, S. *et al.* Determination of Immunoreactive Fraction of Radiolabeled Monoclonal Antibodies: What Is an Appropriate Method? *Cancer Biother. Radiopharm.* **19**, 706–717 (2004).
2. Lindmo, T., Boven, E., Cuttitta, F., Fedorko, J. & Bunn, P. A. Determination of the Immunoreactive Fraction of Radiolabeled Monoclonal Antibodies by Linear Extrapolation to Binding at Infinite Antigen Excess 1. *J. Immunol. Methods* **72**, 77–89 (1984).
3. d’Orchymont, F. & Holland, J. P. Supramolecular Rotaxane-Based Multi-Modal Probes for Cancer Biomarker Imaging. *Angew. Chemie Int. Ed.* (2022). doi:10.1002/anie.202204072